Research on the Application of Vortex Lattice Method and Doublet Lattice Method in Aerodynamic Analysis of the Wing of Solar-Powered Unmanned Aerial Vehicle

Lei Chen[1,*] and *Dmitry* Strelets[1,†]

[1]Moscow Aviation Institute (National Research University), Moscow, Russia

Abstract. In this paper the application of doublet lattice method and vortex lattice method is discussed. A wing of a solar-powered unmanned aerial vehicle (UAV) is chosen as the model. Both the methods are used to calculating the pressure distribution. The results show that the two methods can be used for unsteady aerodynamic analysis of such aircraft in time domain and frequency domain respectively.

1 Introduction

Solar-powered UAV is a kind of aircraft that uses photovoltaic elements to convert the energy of solar radiation into electric energy for maintaining flight and completing scheduled tasks. With no need to land to refuel, such vehicles could theoretically fly permanently. High-altitude solar-powered drones are thought to be a substitute for near-Earth satellites for tasks such as forest fire monitoring and signal transmission in the future. Therefore, in recent years, many countries have developed rapidly stratospheric solar-powered UAV. The Airbus Zephyr S completed 18 consecutive days of flight in 2021, China's Qimingxing-50 solar-powered UAV cruised at an altitude of more than 20,000 meters, and the Phasa-35 developed by Britain's BAE Systems and Prismatic can carry a mission payload of 15kg [1].

High-aspect-ratio composite wings are often used in solar-powered UAVs, and they are faced with more complex atmospheric environment in such altitude, so it is very important to perform aeroelastic analysis [2].

Traditionally, aerodynamic analysis based on potential flow theory and combined with elastic mechanics is used to analyze aeroelasticity of the high aspect ratio solar-powered UAV in engineering. It should be noted that the nonlinear deformation of the wing needs to be processed by the solver to ensure the calculation accuracy.

At present, with the improvement of computer performance, the strong coupling aeroelastic calculation method of computational fluid mechanics and computational structural mechanics by using the supercomputer is also paid attention in the engineering

---

* Corresponding author: lechen@mai.education
† Corresponding author: dimstrelets@rambler.ru

field [3]. However, this method has high hardware requirements and long calculation time, and is not suitable for the initial design stage.

Therefore, application of two important aerodynamic analysis methods of potential flow theory is discussed in this paper.

2 Methodology

2.1 Doublet vortex method

Doublet lattice method (DLM) was first published by Albano and Rodden in 1968 [4]. This method simplifies the aerodynamic process by assuming a fixed harmonic frequency. As a frequency-domain based aerodynamic analysis tool, this method is often used in aeroelastic analysis based on modal coordinates combined with structural dynamics. However, a time domain model can also be established by introducing rational fraction approximation [5].

Dr. Blair's algorithm is used in this article [6], where a planar wing with a limited swept angle in Fig. 1 is considered:
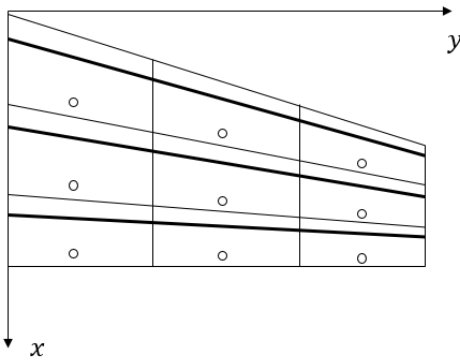

Fig. 1. Arrangement of doublet sheet and control points in a swept planar wing.

Doublet line and the upwash are settled at the 1/4 chord and 3/4 chord position respectively. Furthermore, we assume the pressure difference across a doublet sheet Δp is spatially constant for each box and $\Delta \xi$ as the box chord, which is showed in the Fig. 2.
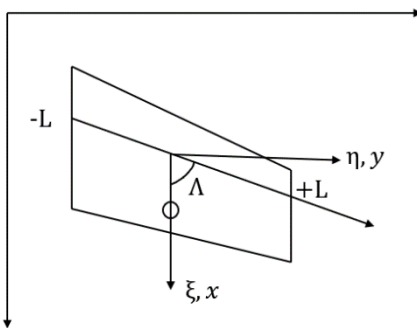

Fig. 2. Local swept coordinate.

In order to get the solution in the frequency domain, we can use the formula of upwash

$$\overline{w}(x, y, 0) = \left[\frac{-\Delta p \Delta \xi}{4\pi\rho U}\right][B_0 + B_1 + B_2] \qquad (1)$$

The definitions of B_0, B_1 and B_2 are given as

$$B_0 = \left[\frac{2LA_0}{y^2 - L^2(sin\Lambda)^2}\right] \qquad (2)$$

$$B_1 = \left[\frac{A_1}{2(sin\Lambda)^2}\right] \ln\left[\frac{(sin\Lambda)^2 L^2 - (2ysin\Lambda)L + y^2}{(sin\Lambda)^2 L^2 + (2ysin\Lambda)L + y^2}\right] + \frac{yA_1}{sin\Lambda}\left[\frac{2L}{y^2 - L^2(sin\Lambda)^2}\right] \qquad (3)$$

$$B_2 = \left[\frac{2LA_2}{(sin\Lambda)^2}\right] + \left[\frac{2yA_2}{sin\Lambda}\right] \ln\left[\frac{(sin\Lambda)^2 L^2 - (2ysin\Lambda)L + y^2}{(sin\Lambda)^2 L^2 + (2ysin\Lambda)L + y^2}\right] + \left[\frac{y^2 A_2}{(sin\Lambda)^2}\right]\left[\frac{2L}{y^2 - L^2(sin\Lambda)^2}\right] \quad (4)$$

A_0, A_1 and A_2 in the formulas above are the complex coefficients used to make complex parabolic approximation of the kernel function, which is the key part of the DLM algorithm:

$$\overline{K}(x_0, y_0, 0) = K_1(x_0, y_0)exp\left[\frac{-i\omega x_0}{U}\right] \qquad (5)$$

Where ω is the hormonic frequency of the motion of the planar wing, U is the steady velocity of the wind. A more detailed calculation method of K_1 is presented in Reference 1.

The parabolic function of l can be written as

$$\overline{K}(x_0, y_0) = A_0 + A_1 l + A_2 l^2 \qquad (6)$$

We identify the coordinates (x_L, y_L), (x_R, y_R) and (x_C, y_C) to represent (x_0, y_0) at $l = -L$, $l = L$ and the midpoint ($l = 0$).

$$A_0 = \overline{K}(x_C, y_C) \qquad (7)$$

$$A_1 = \frac{\overline{K}(x_R, y_R) - \overline{K}(x_L, y_L)}{2L} \qquad (8)$$

$$A_2 = \frac{\overline{K}(x_L, y_L) + \overline{K}(x_R, y_R) - 2\overline{K}(x_C, y_C)}{2L^2} \qquad (9)$$

Thus, we can get the expression of the kernel function

$$\overline{K}(x_0, y_0) = \left[\frac{l(l-L)}{2L^2}\right]\overline{K}(x_L, y_L) + \left[\frac{L^2 - l^2}{L^2}\right]\overline{K}(x_C, y_C) + \left[\frac{l(l+L)}{2L^2}\right]\overline{K}(x_R, y_R) \quad (10).$$

2.2 Unsteady vortex lattice method

Among potential-flow method, the unsteady vortex lattice method (UVLM) is particularly suitable for dynamic analysis [7]. The basis of the method is the modelling of the wing as a thin sheet of vorticity, composed of vortex rings (rectangular, in its simplest version). Additional vortex rings break off at the trailing edge to create a second vorticity to model the wake of the wing.

In this paper we will focus on the method described by Katz and Plotkin [8]. As with the model in DLM, we consider a planar wing below in Fig. 3. The blue wireframe indicates the plane of the wing, and the green – wake vortex rings after the trailing edge of the wing. The borders of the vortex rings are located at a quarter of a chord from each panel, and the collocation points at the 3/4 chord.
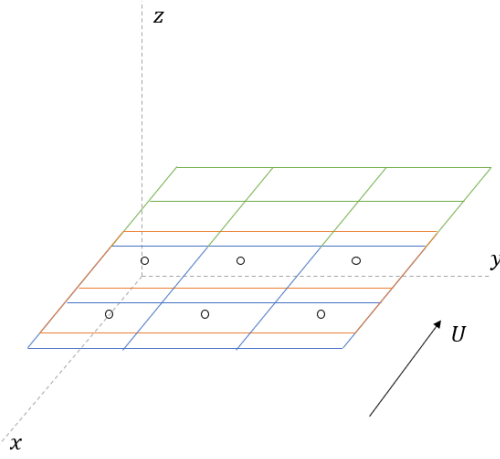
Fig. 3. The arrangement of vortex sheet and collocation points.

The main theorem of UVLM is calculating the intensities of the wing vortex, which can be assumed as a function of time. The intensities of the wake vortex are known since they are equal to the departure vortex of the wing in the previous instants.

The time step is defined as:

$$\Delta t = \frac{c}{m_v U} \tag{11}$$

Where c – length of chord; m_v – number of the wing box in the chord direction; U – velocity of freestream.

Thus, the intensity of the wake vortex rings will be given by

$$\Gamma_{w_{i,j}}(t) = \Gamma_{w_{i-1,j}}(t - \Delta t) \tag{12}$$

The vorticity in the wing at each time step can be calculate by the following equation:

$$\boldsymbol{\Gamma}_b(t) = \boldsymbol{A}_b^{-1}\big(-U\sin\alpha\,\boldsymbol{n}_z - \boldsymbol{A}_w\boldsymbol{\Gamma}_w(t)\big) \tag{13}$$

Where $\boldsymbol{A}_b$ and $\boldsymbol{A}_w$ – aerodynamic influence matrix; α – angle of attack; $\boldsymbol{n}_z$ – normal vector matrix of all the vortex rings.

The integration of the UVLM algorithm in time domain can be finished by the below process:

$\boldsymbol{\Gamma}_b(t - \Delta t)$ and $\boldsymbol{\Gamma}_w(t - \Delta t)$ are known at t time

Use the following formula to solve the propagation of wake $\boldsymbol{\Gamma}_w(t)$:

$$\boldsymbol{\Gamma}_w(t) = \boldsymbol{P}_b\boldsymbol{\Gamma}_b(t - \Delta t) + \boldsymbol{P}_w\boldsymbol{\Gamma}_w(t - \Delta t) \tag{14}$$

Here $\boldsymbol{P}_b$ and $\boldsymbol{P}_w$ are $m_w n_v \times m_v n_v$ matrix (m_w – number of the wake box in the chord direction; n_v - number of the wing box in the wingspan direction

$$\boldsymbol{P}_b = \begin{pmatrix} \boldsymbol{0}_{n_v \times (m_v-1)n_v} & \boldsymbol{I}_{n_v \times n_v} \\ \boldsymbol{0}_{(m_w-1)n_v} & \boldsymbol{0}_{(m_w-1)n_v \times n_v} \end{pmatrix} \tag{15}$$

$$\boldsymbol{P}_w = \begin{pmatrix} \boldsymbol{0}_{n_v \times (m_w-1)n_v} & \boldsymbol{0}_{n_v \times n_v} \\ \boldsymbol{I}_{(m_w-1)n_v} & \boldsymbol{0}_{(m_w-1)n_v \times n_v} \end{pmatrix} \tag{16}$$

Use formula (13) to solve the propagation of wake $\boldsymbol{\Gamma}_b(t)$

Use backward differences to calculate $\dot{\boldsymbol{\Gamma}}_b(t)$:

$$\dot{\boldsymbol{\Gamma}}_b(t) = \frac{\boldsymbol{\Gamma}_b(t) - \boldsymbol{\Gamma}_b(t - \Delta t)}{\Delta t} \tag{17}$$

Use the formulas (18-21) to calculate the difference of pressure, the lift distribution, the total lift and the coefficient of lift at each time step:

$$\Delta p_{i,j}(t) = \rho U cos\alpha \frac{\Gamma_{b_{i,j}}(t)}{\Delta x_{i,j}} + \rho \dot{\Gamma}_{b_{i,j}}(t) \qquad (18)$$

$$\boldsymbol{L}_{i,j}(t) = \left(\rho U cos\alpha \boldsymbol{G}_y \boldsymbol{\Gamma}_b(t) + \rho \boldsymbol{G}_S \dot{\boldsymbol{\Gamma}}_b(t)\right) cos\alpha \qquad (19)$$

$$L(t) = \sum_{i=1}^{M} \sum_{j=1}^{N} L_{i,j}(t) \qquad (20)$$

$$C_L(t) = \frac{L(t)}{\frac{1}{2}\rho U S} \qquad (21)$$

Where S – the square of the wing; and $L_{i,j}(t)$ can be expressed as

$$L_{i,j}(t) = \left(\rho U cos\alpha \Gamma_{b_{i,j}}(t)\Delta y_{i,j} + \rho \dot{\Gamma}_{b_{i,j}}(t)\Delta S_{i,j}\right) cos\alpha \qquad (22)$$

Go to the next temporary step.

3 Numerical simulation and results

3.1 The chose of model and work condition

The wing model of solar-powered UAV with aspect ratio 15 in reference [9] is chosen. The half-wing model is shown in Fig. 4, here the length is 7500mm, and the length of the chord is 1000mm. As a low altitude solar-powered UAV the flight Mach number is set as 0.18 with a 340m/s local sound speed.

In this article we don't discuss the nonlinear deformation of the wing, in another word, the work is just about the linear unsteady aerodynamic analysis.
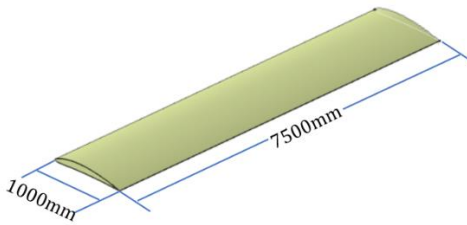

Fig. 4. The model of wing chosen in simulation.

The reduced frequency is considered as 0.34 in the simulation using DLM method, and Theodorsen method is compared with it. The amplitude of the angle of attack is set to 5°and varies with time in sinusoidal mode.

The same speed velocity as jump incoming flow is considered in UVLM simulation. The angle of attack is constant as 5°.

3.2 Results and analysis

The calculation results of pressure coefficient distribution are shown in Fig. 5 (a) and (b). The results show that DLM method has a larger pressure gradient at the leading edge than UVLM method with the same mesh density (chord direction - 20; span direction - 40).
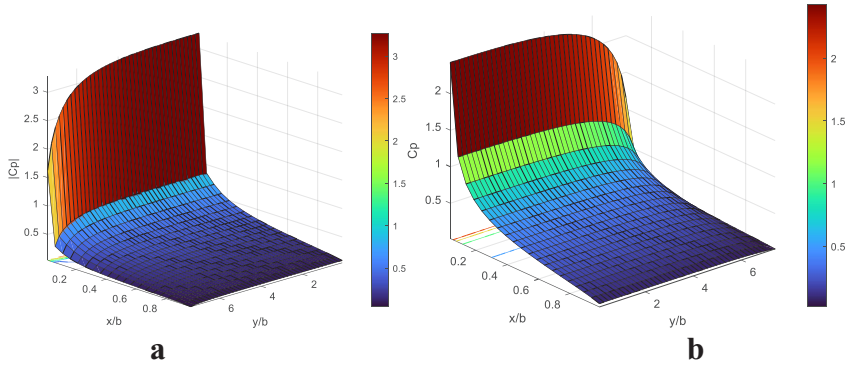
Fig. 5. a. Amplitude distribution of pressure coefficient of half-span, DLM method.

b. Distribution of pressure coefficient of half-span at final time step, UVLM method.
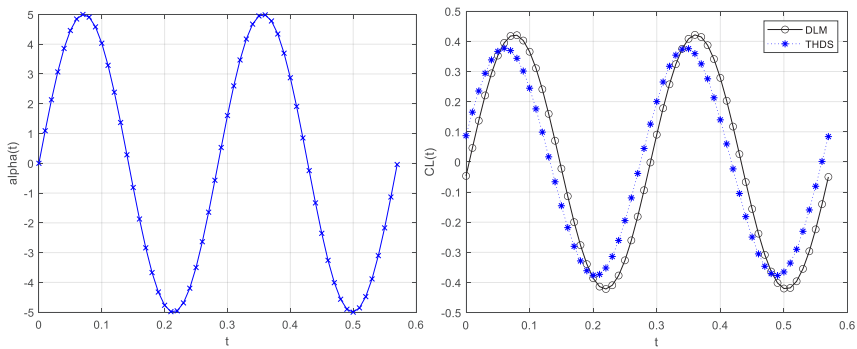

Fig. 6. Variation of angle of attack and oscillation of CL calculated by DLM and Theodorsen method.

Fig.6 shows the oscillation of the angle of attack and the variation of lift coefficient. Obviously, the calculated results of DLM method have phase lag, and the amplitude is larger than the results by Theodorsen method. Compared with the results of DLM method, although there is a larger pressure gradient at the leading edge, the steady-state lift coefficient calculated by UVLM is larger.
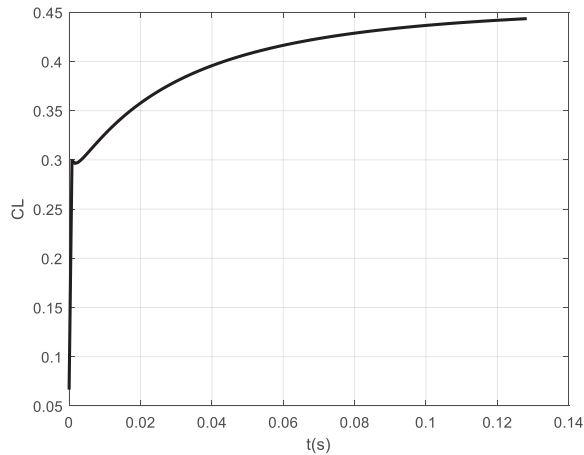
Fig. 7. Variation of lift coefficient over time with jump flow calculated by UVLM.

4 Conclusion

The results show that both DLM and UVLM method can be used for unsteady aerodynamic analysis of solar UAV wings. By comparing with Theodorsen method, it is found that the two methods can get a larger overall lift coefficient. In practical applications, the desired objective should be considered to determine which method should be adopted. It should also be noted that the UVLM method takes longer computation time with the same number of grids.

References

1. M. Wu, L. Su, J. Chen et al, Development and Prospect of Wireless Power Transfer Technology Used to Power Unmanned Aerial Vehicle, Electronics, **11**, 2297 (2022) doi:10.3390/electronics11152297

2. C. Xie, Y. Liu, C. Yang, J.E. Cooper, Geometrically Nonlinear Aeroelastic Stability Analysis and Wind Tunnel Test Validation of a Very Flexible Wing. Shock and Vibration (2016) doi:10.1155/2016/5090719

3. A.G. Bratukhin, S.A. Serebryansky, D.Y. Strelets et al. *Digital technologies in the life cycle of Russian competitive aviation equipment*, Moscow Aviation Institute (National Research University), Moscow, 2020 ISBN 978-5-4316-0694-6. EDN ZGQVGN

4. E. Albano, W.P. Robben, A doublet-lattice method for calculating lift distributions on oscillating surfaces in subsonic flows, AIAA J., **7**(2), 279-285 (1969) doi:10.2514/3/3.5086

5. W. Eversman, A. Tewari, Consistent Rational-Function Approximation for Unsteady Aerodynamics, J. of Aircraft, **28**(9), 545–552 (1991) doi:10.2514/3.46062

6. M. Blair, A Compilation of the Mathematics Leading to the Doublet Lattice Method. Defense Technical Information Center TR WL-TR-92-3028, Belvoir, VA, 1992

7. S. Maraniello, R. Palacios, State-Space Realizations and Internal Balancing in Potential-Flow Aerodynamics with Arbitrary Kinematics. AIAA J., **57**(4), 1-14 (2019) doi:10.2514/1.J058153

8. J. Katz, A. Plotkin, *Low-Speed Aerodynamics* (Cambridge Univ. Press, New York, 2001) doi:10.1017/CBO9780511810329

9. Y. Zhang, Aerodynamic, Structures and Energy Coupled Multi-Objective Optimization for Solar Powered UAV's wing. Dissertation, Beijing Institute of Technology (2015)